Novel Agouti-Related-Protein-Based Melanocortin-1 Receptor Antagonist

Ramanan Thirumoorthy,[†] Jerry Ryan Holder,[‡] Rayna M. Bauzo,[‡] Nigel G. J. Richards,[†] Arthur S. Edison,*[,§] and Carrie Haskell-Luevano*[,‡]

Departments of Chemistry, Medicinal Chemistry, and Biochemistry and Molecular Biology, University of Florida, Gainesville, Florida 32610

Received May 17, 2001

The melanocortin receptors are G-protein coupled receptors (GPCRs) that activate the cAMP signal transduction pathway and are stimulated by the melanocortin agonist α-melanocyte stimulating hormone (α-MSH). Members of these melanocortin receptors are antagonized by agouti (ASP) and agouti-related protein (AGRP), which are the only known endogenous antagonists of GPCRs identified to date. Structure−function studies of the hAGRP(109−118) decapeptide, Tyr-c[Cys-Arg-Phe-Phe-Asn-Ala-Phe-Cys]-Tyr-NH_2, by replacing the 26-membered disulfide Cys^2-Cys^9 ring with lactam bridges resulted in the identification of a novel peripheral skin melanocortin-1 receptor (MC1R) antagonist. This antagonist, Tyr-c[Glu-Arg-Phe-Phe-Asn-Ala-Phe-Dpr]-Tyr-NH_2, possesses a 27-membered ring with the lactam bridge being formed from the Cα-carboxyl moiety of Glu (instead of the typical side chain carboxyl moiety) with the amine of the diaminopropionic acid (Dpr) residue. This mouse MC1 receptor antagonist ($pA_2 = 5.9$) is also an antagonist at the brain melanocortin-4 receptor ($pA_2 = 6.9$), with no observable pharmacology at the melanocortin-3 or -5 receptors. This MC1R hAGRP(109−118) based decapeptide is novel in that AGRP(83−132) itself does not bind to, agonize, or antagonize the skin MC1R. Structural analysis has been performed using two-dimensional ^1H NMR and computer-assisted molecular modeling (CAMM) techniques in attempts to identify structural features of this Tyr-c[Glu-Arg-Phe-Phe-Asn-Ala-Phe-Dpr]-Tyr-NH_2 (cyclo Glu αCOOH-Dpr βNH) peptide that can differentially result in antagonist versus agonist properties at the mMC1R.

Introduction

Agouti-related protein (AGRP) is one of two known naturally occurring antagonists of G-protein coupled receptors (GPCRs) identified to date.[1,2] AGRP was identified on the basis of the sequence similarity to the cysteine-rich C-terminus of agouti (ASP) and found to be expressed in the hypothalamus of rodents[1−3] and primates.[4] A polymorphism in AGRP has been identified in humans diagnosed with anorexia nervosa,[5] linking a human physiological disease state with AGRP. Interestingly, AGRP only antagonizes the brain melanocortin receptors MC3R and MC4R[2,6] and, when ectopically expressed in transgenic mice, does not result in the yellow coat color observed for the agouti mouse,[2,7] physiologically demonstrating in vivo that AGRP does not antagonize the skin melanocortin-1 receptor (MC1R). The melanocortin receptor family consists of five receptors (MC1R−MC5R) identified to date.[8−14] These receptors belong to the superfamily GPCRs that activate the adenylate cyclase signal transduction pathway.[15] The melanocortin peptides (α-, β-, γ-melanocyte stimulating hormones and adrenocorticotropin, ACTH) are the endogenous ligands for these melanocortin receptors and are derived by posttranslational processing of the proopiomelanocortin (POMC) gene transcript. The MC1R is expressed in melanocytes and is involved in coat coloration and pigmentation.[8,11,16] The MC2R only responds to simulation by ACTH, is expressed in the adrenal cortex and adipocytes, and is involved in steroidogenesis.[11] The MC3R is expressed in the brain, heart, placenta, and gut[10−12] and is involved in energy homeostasis.[17,18] The MC4R is expressed primarily in the brain with no detectable expression in peripheral tissues[11,13] and has been demonstrated to be involved in feeding behavior and obesity.[19,20] The MC5R is expressed in muscle, liver, spleen, lung, brain, adipocytes, and a variety of other tissues[14,21] and has been identified as being involved in exocrine gland function.[22]

Only two naturally occurring antagonists of GPCRs have been reported to date (Figure 1). ASP, the first endogenous GPCR antagonist identified,[23] was characterized as antagonizing the skin MC1R and the brain MC4R.[24] These data resulted in the hypothesis that the yellow and obese phenotype of the *agouti* (A^ya) mouse (which ectopically expresses the agouti protein due to a promoter rearrangement)[25] is attributed to antagonism of the respective MC1 and MC4 melanocortin receptors by ASP. The cysteine-rich C-terminus of both agouti and AGRP has been identified as possessing nM antagonistic properties equipotent to the full length peptide,[6,26−30] thus suggesting the key structural and molecular recognition features are located in this domain. The disulfide bond combinations of AGRP, which have been perplexing scientists in the field, have been identified (Figure 1).[31]

Previous structure−activity studies of the agouti peptide identified the importance of the three amino acid motif Arg-Phe-Phe[26,32−34] which is conserved in both agouti and AGRP (Figure 1). A homology molecular

* To whom correspondences should be addressed. For chemistry and pharmacology: C.H.-L., Department of Medicinal Chemistry, P.O. Box 100485. E-mail: Carrie@cop.ufl.edu. For NMR and CAMM: A.S.E., Department of Biochemistry and Molecular Biology, P.O. Box 100245. E-mail: art@ascaris.ufbi.ufl.edu.

[†] Department of Chemistry.

[‡] Department of Medicinal Chemistry.

[§] Department of Biochemistry and Molecular Biology.

10.1021/jm010215z CCC: $20.00
Published on Web 10/18/2001

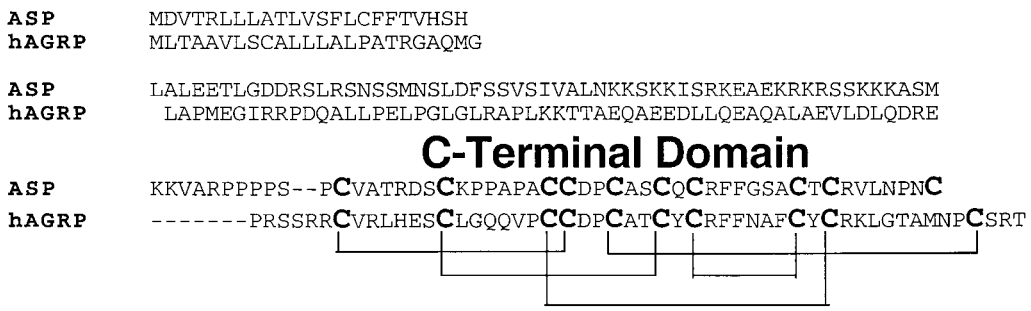

Figure 1. Primary sequence comparison of the only known naturally occurring antagonists of G-protein coupled receptors identified to date, agouti (ASP) and agouti-related protein (AGRP).

Table 1. Functional Activity of The Lactam Derivatives of hAGRP(109−118) at the Mouse Melanocortin Receptors[a]

			mMC1R		mMC4R	
peptide	structure	ring size	agonist EC_{50} (μM)	fold diff	antagonist pA_2	fold diff
hAGRP(109−118)	Tyr-c[**Cys**-Arg-Phe-Phe-Asn-Ala-Phe-**Cys**]-Tyr-NH_2	26	5.12 ± 3.04	1	6.81 ± 0.24	1
1	**Tyr-c[Asp**-Arg-Phe-Phe-Asn-Ala-Phe-**Dpr**]-Tyr-NH_2	26	5.96 ± 2.51	1	6.32 ± 0.15	3
2	**Tyr-c[Glu**-Arg-Phe-Phe-Asn-Ala-Phe-**Dpr**]-Tyr-NH_2	27	$pA_2 = 5.92 \pm 0.11$	Antagonist	6.98 ± 0.07	1.5
3	**Tyr-c[Dpr**-Arg-Phe-Phe-Asn-Ala-Phe-**Asp**]-Tyr-NH_2	25	28.1 ± 12.8	5	5.84 ± 0.22	9

[a] The indicated errors represent the standard errors of the mean determined from at least three or more independent experiments. The antagonists were determined using the Schild analysis with the melanocortin agonist MTII (Ac-Nle-c[Asp-His-DPhe-Arg-Trp-Lys]-NH_2) being used. The fold difference of the antagonists were determined by converting the pA_2 value to the Ki value where Ki = − log pA_2.

model of agouti, based upon the NMR structures of ω-conotoxin GVIA and ω-agatoxin IVB, was generated which allowed for the visualization of how these antagonist Arg-Phe-Phe residues may be mimicking the melanocortin α-MSH agonist Phe-Arg-Trp residue interactions with the melanocortin receptors.[32] The His-Phe-Arg-Trp residues in the melanocortin agonist ligands have been identified as important for melanocortin receptor stimulation.[35−41] More recently, the first structural study of the NMR structure for the C-terminal AGRP region has been reported.[33] Additionally, we have identified the AGRP derived decapeptide Yc[CRFFNAFC]Y as possessing agonist activity at the skin MC1R, providing experimental support for the hypothesis that the antagonist Arg-Phe-Phe motif may be mimicking the melanocortin agonist Phe-Arg-Trp molecular interactions with the melanocortin receptors.[42]

The current study was undertaken to identify AGRP based decapeptides that could be converted from skin mMC1R agonists to mMC1R antagonists and determine the structural properties of these MC1R agonists and antagonists using ^{1}H two-dimensional (2D) NMR and computer-assisted molecular modeling (CAMM) techniques.

Results

Pharmacology. The peptides examined in this study are derived from the hAGRP(109−118)[42,43] sequence and have the disulfide bridge replaced by a lactam bridge between Asp or Glu and Dpr. Figure 2 illustrates the primary structures of the three peptides reported herein where the lactam bridge is formed using the Cα carboxylic acid of Asp or Glu instead of the typical side chain carboxylic acid moiety. Table 1 summarizes the pharmacology of the compounds examined in this study at the mouse melanocortin MC1 and MC4 receptors. These compounds were also evaluated at the mMC3 and mMC5 receptors but did not result in agonist or antagonist activities (data not shown). The 26-membered ring substituting a lactam bridge (peptide **1**) for a disulfide bridge hAGRP(109−118) resulted in equipotent mMC1R agonist activities and only a 3-fold difference in antagonist potencies at the mMC4R (within experimental error of these assays). Surprisingly, peptide **2** which possesses a 27-membered lactam ring composed of the Glu and Dpr amino acid (Figure 2) resulted in a MC1R antagonist (Figure 3). Peptide **3**, a 25-membered ring between Dpr and Asp, resulted in a 5-fold decreased mMC1R agonist potency and 9-fold decreased antagonist mMC4R potency, compared with hAGRP(109−118).

Nuclear Magnetic Resonance. The chemical shifts of each of the peptides in this study were assigned using standard TOCSY and NOESY ^{1}H-based strategies (see Supporting Information).[44] This approach utilizes TOCSY spectra to identify resonances within a given amino acid and NOESY spectra to correlate one amino acid with the next through interactions of the α and/or β protons of residue i with the amide proton of residue $i + 1$. This strategy allowed the complete assignment of all amino acids, including lactam bridges and the nonstandard orientations of Asp and Glu. The aliphatic "fingerprint" and amide to amide regions of 750 MHz NOESY spectra of each peptide are shown in Figure 4.

Despite the fact that the three peptides are similar chemically (Figure 2), the NMR spectra and NOE patterns of connectivity are surprisingly different (Figure 4). NMR chemical shifts are extremely sensitive to the electronic environment and thus provide useful probes into changes in molecular structure. However, a quantitative interpretation of chemical shifts from small, flexible peptides is currently impossible, because they are so sensitive to small changes in structure and represent a population-weighted average of rapidly interconverting structures with different chemical shifts. Moreover, most analyses of peptide or protein chemical shift values are from aqueous solvents and not mixtures of acetonitrile and water, as in the current study. We

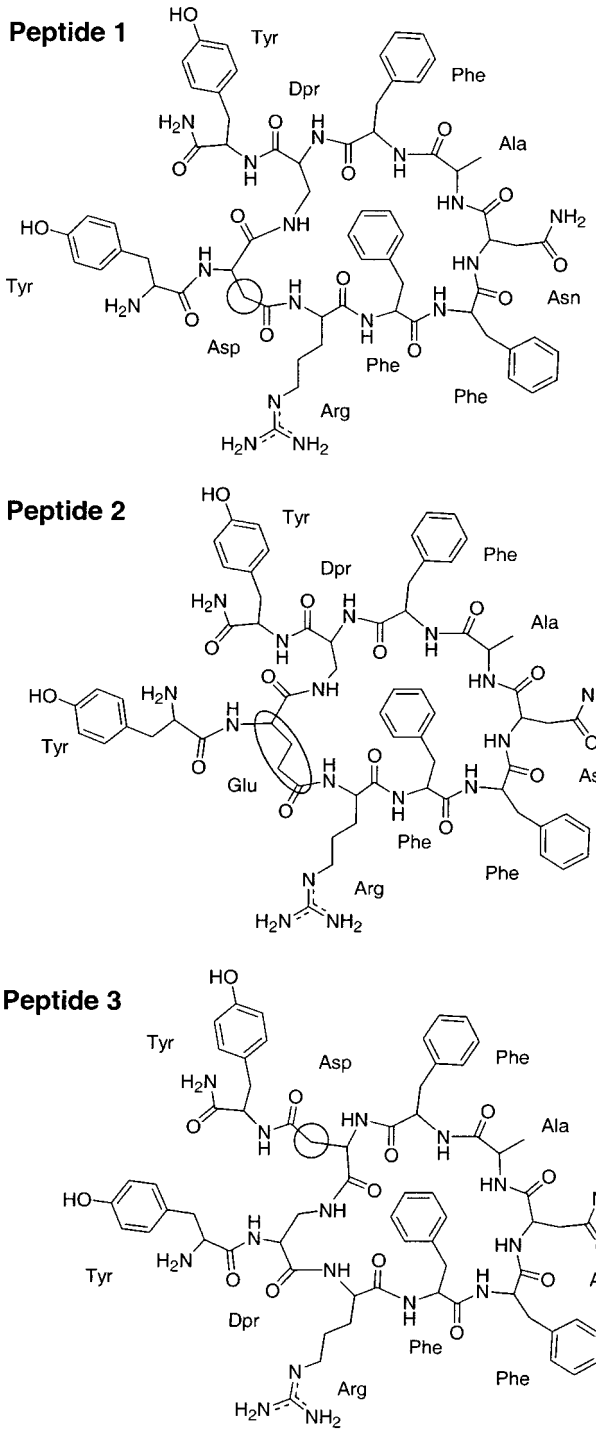

Figure 2. Primary structure of peptide **1** (26-membered ring), peptide **2** (27-membered ring), and peptide **3** (25-membered ring) illustrating the location of the Asp or Glu side chain (circled) in relationship to the lactam bridge.

can, however, make a qualitative comparison of the backbone ^{1}H shifts in the peptides in this study by subtracting a common reference value from each shift. Figure 5 is a histogram of differences between experimental and aqueous random-coil chemical shifts[45] for the conserved Arg-Phe-Phe-Asn-Ala-Phe region of the three peptides in this study. It is impossible to assess the degree of well-ordered structure implicit in the chemical shift data, since random-coil shifts from pure water and 83% acetonitrile 17% water are certain to be different. We can, however, compare shifts of the same

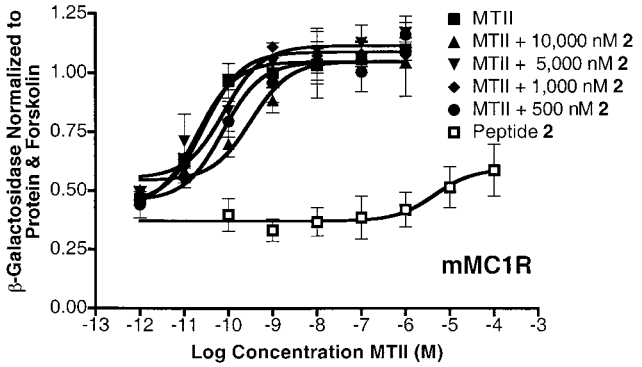

Figure 3. Illustration of peptide **2** (Tyr-c[Glu-Arg-Phe-Phe-Asn-Ala-Phe-Dpr]-Tyr-NH_2, 27-membered ring) as an antagonist at the mouse melanocortin-1 receptor. The assay was performed using the Schild analysis and the MTII (Ac−Nle-c[Asp-His-DPhe-Arg-Trp-Lys]-NH_2) melanocortin agonist. Peptide **2** resulted in an antagonist pA_2 value of 5.92 which corresponds to a Ki value of 1.2 μM potency.

amino acid type and the global patterns from one peptide to another. Each sequence has three common Phe residues, and it is clear from Figure 6 that the chemical shifts of these residues can differ significantly, both within a peptide and between peptides. Finally, given that each of the histograms in Figure 5 represent exactly the same common amino acids and that the difference between the peptides is only a methylene group or the orientation of the lactam bridge, there is a remarkable dissimilarity between the groups. We conclude from the dissimilarities that each peptide leads to a unique ensemble of conformations.

Following resonance assignments, we next quantitatively determined three NMR parameters for conformational modeling studies: NOEs, *J*-couplings, and amide proton temperature coefficients. Each of these parameters is sensitive to different structural changes. NOEs provide an estimate of the distance between pairs of protons closer than about 5 Å in space. *J*-couplings are sensitive to dihedral angle according to the well-known Karplus equation.[46] Finally, amide temperature coefficients are complicated and poorly understood, but groups with low values are typically involved in internal H-bonds.[47,48] Figure 6 provides a summary of the NOE, *J*-coupling, and temperature coefficient (TC) data for each of the peptides in this study. The C-terminus of each peptide has similar patterns of NOEs, with several $i - i + 2$ or $i - i + 3$ interactions. Moreover, the Ala residues, which are also involved in several of the longer-range NOEs, each have small $J_{HN,H\alpha}$ couplings. Finally, the variable C-terminal amino acids involved with the lactam bridges all have small temperature coefficients. All of these patterns are consistent with a type I reverse-turn formation in the C-terminal regions.[48] In contrast, each peptide appears to have different conformations in the N-termini. All three structural parameters from peptide **1**, suggest that the center of the molecule around the "Phe-Phe-Asn" site is ordered and likely possesses an additional reverse turn. Peptide **2**, in contrast, has very few NOEs in the central "Phe-Phe-Asn" region, and the *J*-couplings and temperature coefficients from that region have intermediate (and uninformative) values. Peptide **2** does have NOE and temperature coefficient evidence for a reverse turn near the N-terminus in the "Glu-Arg-Phe"

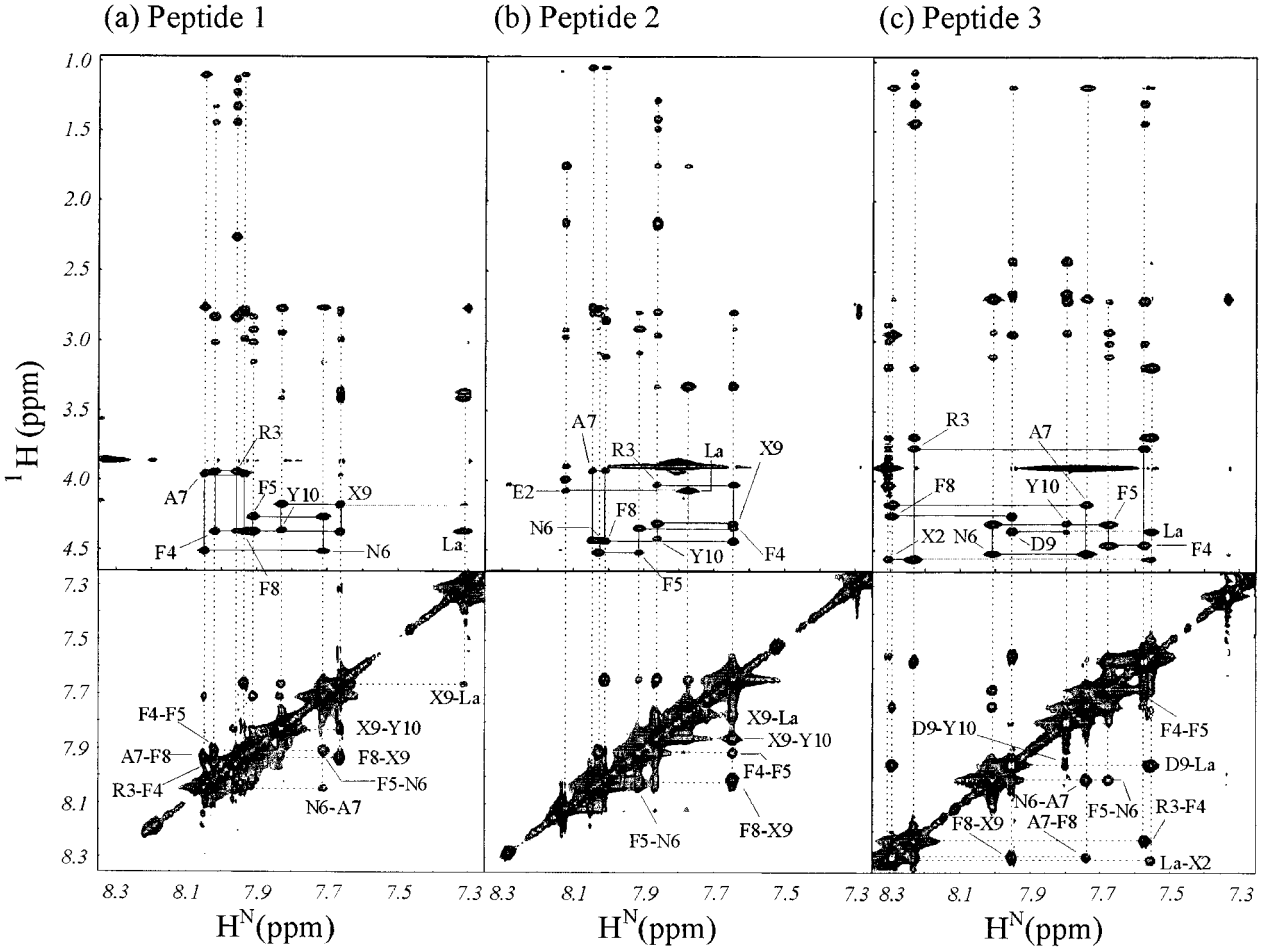

Figure 4. Amide to aliphatic (top) and amide to amide (bottom) regions of NOESY spectra of (a) peptide **1**, (b) peptide **2,** and (c) peptide **3**. The sequential assignments are indicated in the top panels with the amino acid labels referring to the position of the corresponding amide protons, and amide to amide cross-peaks are indicated in the lower panel. The data were collected on a Bruker Avance 750 MHz at 4 °C with a mixing time of 400 ms. The residues labeled "X" are Dpr and "La" are lactams.

residues; however, peptide **3** appears to have the reverse turn shifted to the extreme N-terminus.

Restrained Molecular Dynamics Simulations. To examine the conformational differences between the AGRP peptides, the NMR NOE and *J*-coupling data shown in the Supporting Information were used as pseudo potentials in restrained molecular dynamics (RMD) simulations. Interatomic distances were calibrated from NOESY spectra, as described in the Experimental Section, and flat-bottomed harmonic pseudo potentials were created from the NOE-based distances by adding 1.0 Å to the experimental distance. Backbone ϕ dihedral angles were estimated using the Karplus equation[46,49] and experimental *J*-couplings that were smaller than 5.0 Hz. Flat-bottomed torsional harmonic pseudo potentials were created by adding 30° to each side of the experimental value for ϕ. Linear peptides were first energy minimized, cyclized by forming the lactam bridges, and energy minimized a second time, all with no pseudo potentials. Next, the pseudo potentials were added and RMD simulations were done for at least 20 ns at 500 K in order to attempt to sample all accessible conformations. Following the RMD simulations, structures from 200 equally spaced points along the dynamics trajectory were energy minimized and analyzed.

For each analogue, a superposition of all 200 energy minimized conformations was not distinguishable, suggesting that the simulations each contained multiple conformations. The energy minimized conformations were clustered into families using the computer program XCluster.[50] The clustering was done by comparing the backbone ϕ and ψ dihedral angles of the Arg-Phe-Phe-Asn-Ala-Phe amino acids in the rings of each peptide, and the results are shown in Figure 7. All clustered families with a population of 4 or more conformations (e.g. ≥2% of the total) were considered for further analysis. Peptide **1** possessed 9 families with populations greater than 2% of the total, with the largest family having 18% of the sampled conformations. Peptide **3** possessed 6 families above the cutoff, with the largest family having 20% of the sampled conformations. In contrast, the mMC1R peptide **2** possessed 16 families, with the most populated having only 7% of the population and most families consisting of only 2−4% of the total populations. This result is consistent with the number of NMR restraints used for these peptides (Supporting Information). The MC1R antagonist, **2**, had fewer restraints, suggesting a more flexible structure. Representative dihedral angles and their corresponding populations for each cluster family are given in the Supporting Information.

A representative structure was picked from each populated family in each peptide. The ϕ and ψ angles of the representative structures (Supporting Information) were checked for reverse turns, as indicated by

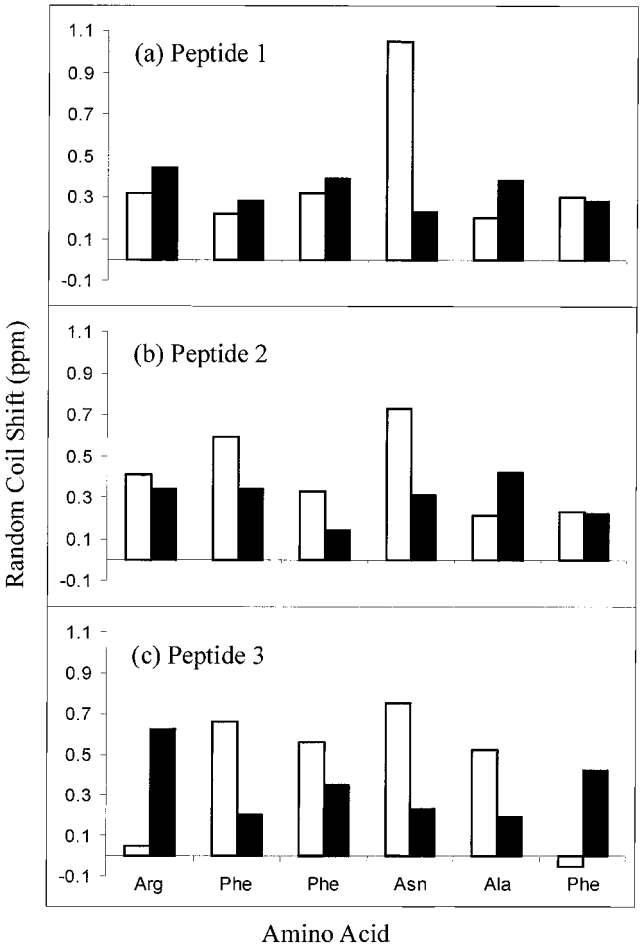

Figure 5. Histogram of the difference between the random coil and experimental chemical shifts of (a) peptide **1**, (b) peptide **2**, and (c) peptide **3**. The amide and α protons are represented by white bars and black bars, respectively.

NMR data. Some of the representative structures for peptides **1** and **2** have a type I β-turn with the central residues Ala[7] and Phe[8]. In contrast, some representative structures of peptide **3** have the same turn shifted to residues Asn[6] and Ala[7].

Consistent with the NMR data, most of the representative structures of **1** and **3** have hydrogen bonds between backbone carbonyl groups and only those amide protons that had low experimental temperature coefficients. In **2**, the Dpr residue is hydrogen bonded in most conformers, as predicted by a low-temperature coefficient. However a few low-population peptide **2** conformers have hydrogen bonds to amide protons that did not have low-temperature coefficients. The different conformers have different hydrogen bonds and do not contribute significantly to the bulk temperature coefficients.

Because each peptide in the study is slightly different, we were unable to do a full cluster analysis on all of the 600 conformations from all three peptides. To compare conformations between the different peptides, we created linear (Gly)9 peptides (in silico) and entered the ϕ and ψ angles for each of the populated conformations shown in Tables 3−5 of the Supporting Information from each of the peptides. These (Gly)9 peptides were then clustered with XCluster as described above and shown, along with backbone superimpositions of the representative structures, in Figure 8. With one exception, the major families of **3** are very similar, as indicated by the large blue regions in Figure 7c and the blue region in the lower right-hand corner of Figure 8. However, most of the peptide **3** conformers bear little similarity to conformers from the other two peptides. Interestingly, the **3** conformer that is dissimilar to other **3** conformers is somewhat similar to two conformers from peptide **2** and one conformer from peptide **1**, as indicated by the light blue boxes in Figure 8. In contrast to **3,** peptides **1** and **2** each have fewer similarities within each peptide but have a significant number of conformers that are similar between the two peptides. Finally, the region of Figure 8 that clearly shows the least amount of similarity is between analogues **1** and **3**, the two MC1R agonists.

Discussion

AGRP has been pharmacologically demonstrated to antagonize the brain melanocortin receptors (MC3R and MC4R), while neither binding to nor antagonizing the peripheral skin melanocortin receptor, MC1R.[6] In vivo, in the overexpressing AGRP transgenic mouse, AGRP was characterized as not antagonizing the skin MC1R as a normal coat color phenotype resulted.[2,7] Interestingly, the hAGRP(109−118) decapeptide, Tyr-c[Cys-Arg-Phe-Phe-Asn-Ala-Phe-Cys]-Tyr-NH_2, has been characterized as possessing agonist activity at the mMC1R.[42] Herein, we have identified a hAGRP(109−118) derivative that can now antagonize the skin MC1R.

In addition to the endogenous MC1R antagonist agouti,[24] frog skin (putative MC1R) melanocortin-based antagonists have been reported.[51−54] The peptide Ac-Nle-Asp-Trp-DPhe-Nle-Trp-Lys-NH_2 is a derivative of NDP-MSH (Ac-Ser-Tyr-Ser-Nle-His-DPhe-Arg-Trp-Gly-Lys-Pro-Val-NH_2) that is reported to have an antagonist pA_2 value of 8.4 (3 nM potency) using the classical *Rana pipiens* frog skin bioassay.[51] Based upon the α-MSH sequence Glu-His-Phe-Arg-Trp-Gly-Lys-Pro-Val-NH_2, several combinatorial chemistry peptide libraries were synthesized on the basis of 7, 8, or 9 of these amino acids (counting form the C-terminus), and greater than 12 linear antagonists were identified with the reported most potent, based upon its binding affinity, consisting of the Met-Pro-DPhe-Arg-DTrp-Phe-Lys-Pro-Val-NH_2 sequence.[52] A separated study of tripeptide libraries resulted in the identification of the DTrp-Arg-Leu-NH_2 as an antagonist of the *Xenopus laevis* by direct administration onto the frog skin,[53] although this was not reproducible in the *Rana pipiens* frog skin bioassay (Haskell-Luevano, C.; Hruby, V. J.; Hadley, M. E. Unpublished results). These antagonists were identified using a novel diffusion assay and *Xenopus laevis* (frog) dermal melanophores. These melanocortin-based peptide antagonists are all linear, and other than being antagonists of the putative frog skin MC1R, they share no sequence similarity with the AGRP decapeptide mouse MC1R antagonist Tyr-c[Glu-Arg-Phe-Phe-Asn-Ala-Phe-Dpr]-Tyr-NH_2, peptide **2**, described herein. Two derivatives of the cyclic MTII (Ac-Nle-c[Asp-His-DPhe-Arg-Trp-Lys]-NH_2) agonist, SHU8914 (Ac-Nle-c[Asp-His-(pI)DPhe-Arg-Trp-Lys]-NH_2), and SHU9119 (Ac-Nle-c[Asp-His-DNal(2′)-Arg-Trp-Lys]-NH_2) possessed antagonistic properties ($pA_2 \geq 10.3$) in the *Rana pipiens* frog skin assay (putative MC1R), but possessed agonist

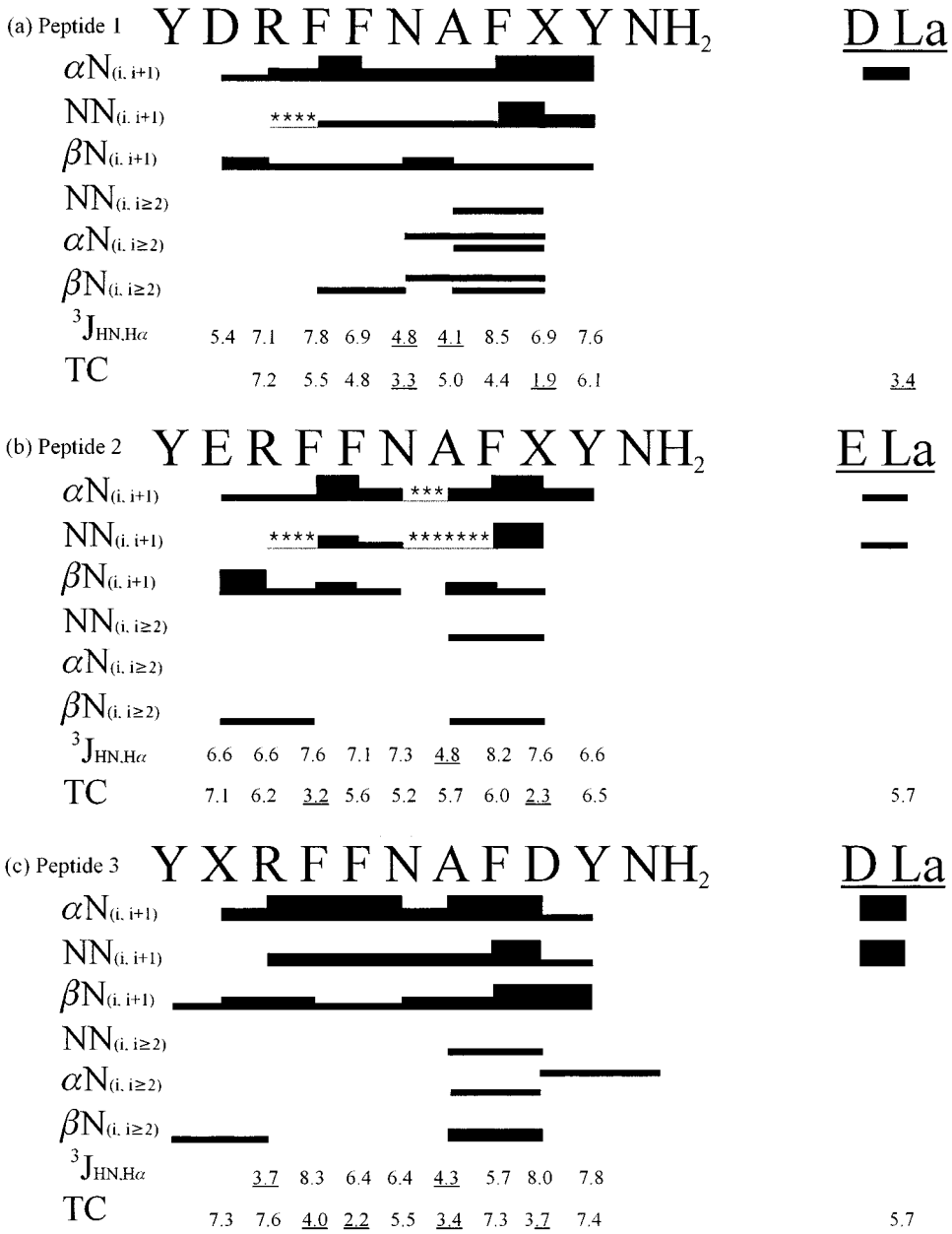

Figure 6. Summary of the NOEs from 400 ms NOESY data for (a) peptide **1**, (b) peptide **2**, and (c) peptide **3**. The residues labeled "X" are Dpr and "La" are lactams. The height of the bar indicates the strength of the NOE, and the asterisked line indicates overlapping NOEs. The $^3J_{HN,H\alpha}$ values indicate scalar coupling constants in hertz. The temperature coefficients (TC) are in units of −ppb°C and represent the slope of the change in amide proton chemical shift with temperature.

activity (55 and 36 nM, respectively) at the cloned human skin MC1R.[54]

The three AGRP-based compounds reported herein differ only in ring size and in the orientation of the lactam bridge. Reversing the standard orientation of the Asp and Glu residues involved in the lactam bridges allowed us to easily change the ring size without changing any of the amino acids used in synthesis. Peptides **1** and **2** differ only by the addition of a single methylene group in **2**, and the orientation of the lactam is the same for both peptides. This single methylene completely changes the pharmacology, the NMR spectral parameters, and the resulting conformational families. In particular, the chemical shifts of the common (Arg-Phe-Phe-Asn-Ala-Phe) residues differ for each peptide (Figure 6), and the patterns of NOEs, *J*-couplings, and temperature coefficients suggest different locations and populations of reverse turns in each peptide (Figure 6). In contrast, peptides **1** and **3** are made from the same amino acids, but because of the placement of the Asp side chain (Figure 2), the ring size is reduced by one methylene in **3**, and the lactam bridge is in a different orientation. Thus, strictly on the basis of chemical similarity, one might predict that peptides **1** and **2** would have similar properties and that these would differ from **3**. However, this prediction was not correct, as **3** and **1** are both agonists of MC1R, and **2** is an antagonist at the same receptor.

Conclusions

This is the first report of a novel cyclic decapeptide melanocortin-1 receptor antagonist that is based upon the endogenous antagonist AGRP sequence that normally only interacts with the brain melanocortin-3 and -4 receptors and not the skin melanocortin receptor (MC1R). The cyclic decapeptide Tyr-c[Glu-Arg-Phe-Phe-

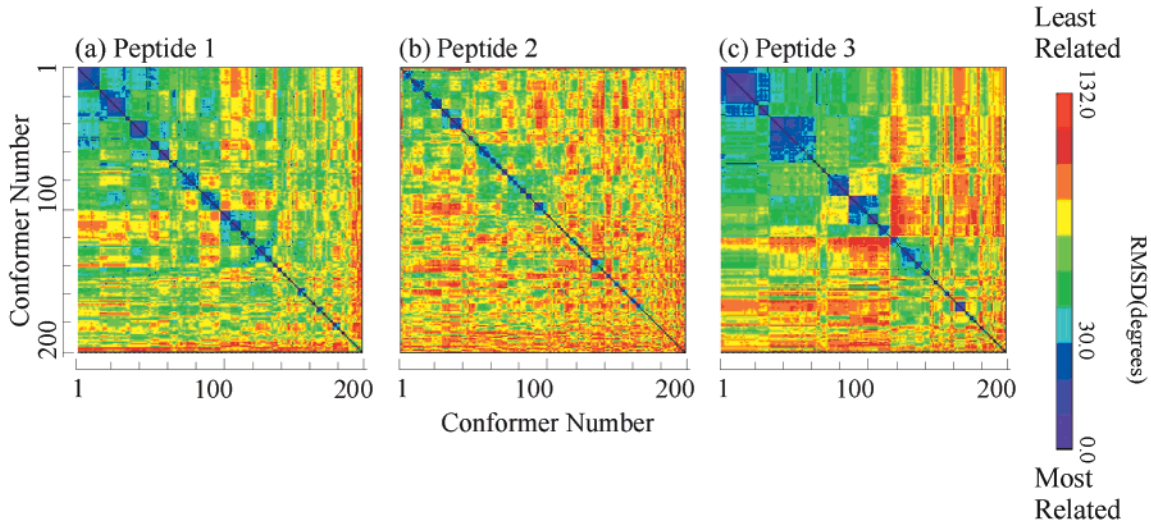

Figure 7. Cluster map of 200 energy minimized conformations of (a) peptide **1**, (b) peptide **2**, and (c) peptide **3**. The clustering was done by comparing the backbone (ϕ and ψ) dihedral angles of the amino acids in the ring of each peptide. The input structures were reordered into groups of similar structures. The first structure from the input list defined the first cluster, and subsequent clusters were formed sequentially from the remaining input list structures. The conformations in the region shaded with blue (dihedral RMSD ≤ 30°) are closely related to each other and form a family, while those shaded from green to red are least related.

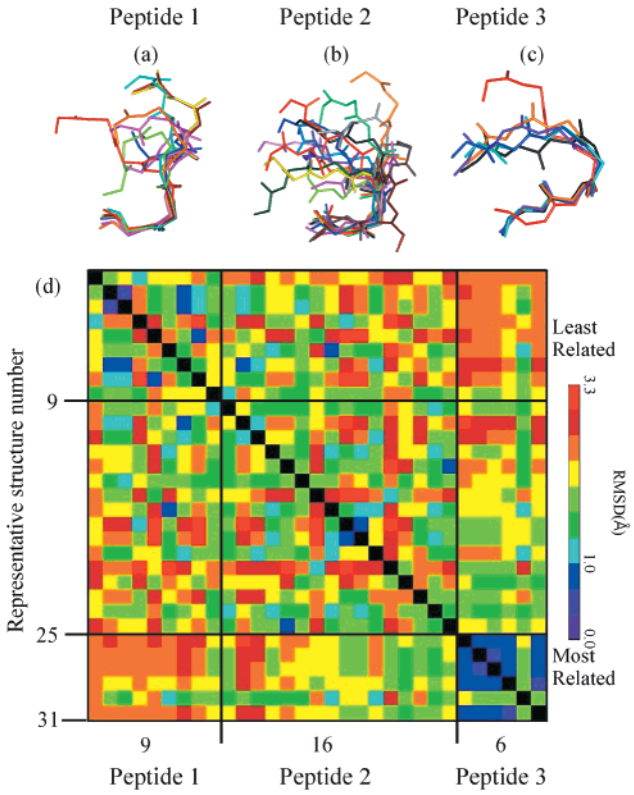

Figure 8. Representative structures of the common residues of each family of (a) peptide **1**, (b) peptide **2**, and (c) peptide **3**. One conformation was found in all three peptide families, shown in red, within each of the backbone molecular structures. In the cluster map of the representative structures (d), the regions shaded with blue (atomic RMSD ≤ 1.0 Å) are closely related to each other, while those shaded from green to red are least related. The clustering was done by comparing the backbone atomic coordinates of the amino acids in the ring of each peptide.

Asn-Ala-Phe-Dpr]-Tyr-NH_2 provides a novel template for further structure−activity studies of antagonists at the skin MC1R. Biophysical and computer modeling studies of the peptides presented herein did not result in any conclusive structural hypothesize attributed for the mMC1R antagonism of the cyclic decapeptide Tyr-c[Glu-Arg-Phe-Phe-Asn-Ala-Phe-Dpr]-Tyr-NH_2.

Experimental Section

Peptide synthesis was performed using standard Boc methodology[55] on an automated synthesizer (Advanced ChemTech 440MOS, Louisville, KY). The amino acids Boc-Tyr(2ClBzl), Boc-Dpr(Fmoc), Boc-Asp(Nα carboxyl-OFm), Boc-Arg(Tos), Boc-Phe, Boc-Asn, and Boc-Ala were purchased from Bachem. The peptides were assembled on pMBHA resin (0.28 meq/g substitution), purchased from Peptides International (Louisville, KY). All reagents were ACS grade or better. The synthesis was performed using a 40 well Teflon reaction block with a course Teflon frit. Approximately 200 mg of resin (0.08 mmol) was added to each reaction block well. Each peptide was synthesized in two separate reaction wells due to reaction volume limitations. The resin was allowed to swell for 2 h in 5 mL of dimethylformamide (DMF) and deprotected using 4 mL of 50% trifluroacetic acid (TFA) and 2% anisole in dichloromethane (DCM) for 3 min followed by a 20 min incubation at 500 rpms, and washed with DCM (4.5 mL, 2 min, 500 rpms 3 times). The peptide−resin salt was neutralized by the addition of 4 mL of 10% diisopropylethylamine (DIEA) in DCM (3 min, 500 rpms, 2 times) followed by a DCM wash (4.5 mL, 2 min, 500 rpms 4 times). A positive Kaiser[56] test resulted, indicating free amine groups on the resin. The growing peptide chain was added to the amide−resin using the general amino acid cycle as follows: 500 μL of DMF is added to each reaction well to "wet the frit," 3-fold excess amino acid starting from the C-terminus is added [400 μM of 0.5 M solution in 0.5 M *N*-hydroxybenzotriazole (HOBt) in DMF] followed by the addition of 400 μL of 0.5 M *N*,*N*′-diisopropylcarbodiimide (DIC) in DMF, and the reaction well volume is brought up to 3 mL using DMF. The coupling reaction is mixed for 1 h at 500 rpms, followed by emptying of the reaction block by positive nitrogen gas pressure. A second coupling reaction is performed by the addition of 500 μL of DMF to each reaction vessel, followed by the addition of 400 μL of the respective amino acid (3-fold excess), 400 μL of 0.5 M *O*-benzotriazolyl-*N*,*N*,*N*′,*N*′-tetramethyluronium hexafluorophosphate (HBTU), 300 μL of 1 M DIEA, the reaction well volume is brought up to 3 mL with DMF, and mixed at 500 rpm for 1 h. After the second coupling cycle, the reaction block is emptied and the resin-Nα-protected peptide is washed with DCM (4.5 mL 4 times). Nα-Boc deprotection is performed by the addition of 4 mL of 50% TFA and 2% anisole in DCM and mixed for 5 min at 500 rpms followed by a 20 min deprotection at 500 rpms. The reaction

Table 2. Analytical Data for the Peptides Synthesized in This Study[a]

peptide	structure	HPLC k' syst 1	HPLC k' syst 2	purity (%)	mass spectral analysis (M + 1)
1	Tyr-c[**Asp**-Arg-Phe-Phe-Asn-Ala-Phe-**Dpr**]-Tyr-NH_2	4.8	10.7	>98	1308.6
2	Tyr-c[**Glu**-Arg-Phe-Phe-Asn-Ala-Phe-**Dpr**]-Tyr-NH_2	5.1	11.3	>95	1324.1
3	Tyr-c[**Dpr**-Arg-Phe-Phe-Asn-Ala-Phe-**Asp**]-Tyr-NH_2	4.6	10.1	>96	1308.2

[a] HPLC k' = [(peptide retention time − solvent retention time)/solvent retention time] in solvent system 1 (10% acetonitrile in 0.1% trifluroacetic acid/water and a gradient to 90% acetonitrile over 40 min) or solvent system 2 (10% methanol in 0.1% trifluroacetic acid/water and a gradient to 90% methanol over 40 min). An analytical Vydac C_{18} column (Vydac 218TP104) was used with a flow rate of 1.5 mL/min. The percentage peptide purity is determined by HPLC at a wavelength of 214λ.

well is washed with 4.5 mL of DCM (4 times), neutralized with 10% DIEA (3 min, 500 rpms, 2 times) followed by a DCM wash (4.5 mL, 2 min, 500 rpms 4 times), and the next coupling cycle is performed as described above. The side chain lactam bridge is formed between the Asp Cα-carboxyl moiety (instead of the common lactam bridge incorporating the Asp side chain carboxy group) and the β amine group of Dpr. The Fmoc and OFm protecting groups are removed from Dpr and Asp or Glu, respectively, by treatment with 4.5 mL of 25% piperidine in DMF (20 min at 500 rpm) with a positive Kaiser test resulting. The lactam bridge between the Asp and Dpr amino acids is formed using 5-fold excess benziotriazolyloxytris(dimethylamino)phosphonium hexafluorophosphate (BOP) and 6-fold excess DIEA as coupling agents and mixing at 500 rpms. The lactam bridges were formed (negative Kaiser test) after approximately 4−5 days at room temperature and 3 days at 36 °C. Deprotection of the remaining amino acid side chains and cleavage of the amide−peptide from the resin was performed by incubation the peptide−resin with anhydrous hydrogen fluoride (HF, 5 mL, 0 °C, 1 h) and 5% *m*-cresol, 5% thioanisole as scavengers. After the reaction is complete and the HF has been distilled off, the peptide is ether precipitated (50 mL × 1) and washed with 50 mL cold (4°) anhydrous ethyl ether. The peptide is filtered off using a course frit glass filter and dissolved in glacial acetic acid, frozen, and lyophilized. The crude peptide yields ranged from 60 to 90% of the theoretical yields. A 40 mg sample of crude peptide was purified by RP-HPLC using a Shimadzu chromatography system with a photodiode array detector and a semipreparative reversed-phase high-performance liquid chromatography (RP-HPLC) C_{18} bonded silica column (Vydac 218TP1010, 1.0 × 25 cm) and lyophilized. The purified peptide was >95% pure as determined by analytical RP-HPLC and had the correct molecular mass (University of Florida protein core facility), Table 2.

Cell Culture and Transfection. Briefly, HEK-293 cells were maintained in Dulbecco's modified Eagle's medium (DMEM) with 10% fetal calf serum and seeded 1 day prior to transfection at (1−2) × 10^6 cell/100 mm dish. Melanocortin receptor DNA in the $pCDNA_3$ expression vector (20 μg) were transfected using the calcium phosphate method. Stable receptor populations were generated using G418 selection (1 g/mL) for subsequent bioassay analysis.

Functional Bioassay. HEK-293 cells stably expressing melanocortin receptors were transfected with 4 μg of CRE/β-galactosidase reporter gene as previously described.[57,58] Briefly, 5000−15 000 posttransfection cells were plated into 96 well Primera plates (Falcon) and incubated overnight. At 48 h posttransfection the cells were stimulated with 100 μL of peptide (10^{-4}−10^{-10} M) or forskolin (10^{-4} M) control in assay medium (DMEM containing 0.1 mg/mL of BSA and 0.1 mM isobutylmethylxanthine) for 6 h. The assay media were aspirated, and 50 μL of lysis buffer (250 mM Tris-HCl pH = 8.0 and 0.1% Triton X-100) was added. The plates were stored at −80° overnight. The plates containing the cell lysates were thawed the following day. Aliquots of 10 μL were taken from each well and transferred to another 96-well plate for relative protein determination. To the cell lysate plates, 40 μL of phosphate-buffered saline with 0.5% BSA was added to each well. Subsequently, 150 μL of substrate buffer (60 mM sodium phosphate, 1 mM $MgCl_2$, 10 mM KCl, 5 mM β-mercaptoethanol, 200 mg ONPG) was added to each well, and the plates were incubated at 37°. The sample absorbance, OD_{405}, was measured using a 96-well plate reader (Molecular Devices). The relative protein was determined by adding 200 μL of 1:5 dilution Bio Rad G250 protein dye:water to the 10 μL cell lysate sample taken previously, and the OD_{595} was measured on a 96-well plate reader (Molecular Devices). Data points were normalized both to the relative protein content and nonreceptor-dependent forskolin stimulation. The antagonistic properties of these peptides were determined by the ability of these ligands to competitively displace the MTII agonist (Bachem) in a dose-dependent manner. The pA_2 values were generated using the Schild analysis method.[59]

Data Analysis. EC_{50} and pA_2 values represent the mean of duplicate experiments performed in triplicate, quadruplet, or more independent experiments. EC_{50} and pA_2 value estimates and their associated standard errors were determined by fitting the data to a nonlinear least-squares analysis using the PRISM program (v3.0, GraphPad Inc.). The results are not corrected for peptide content.

NMR Spectroscopy. (See Supporting Information for data tables.) NMR samples were prepared by dissolving 1.0−1.3 mg of the purified peptides in a 550 μL solution of 82% (v/v) acetonitrile-d_3 (Cambridge Isotope Labs, 99% enriched) and 18% H_2O. NMR data were collected using Bruker Avance spectrometers operating at 600 and 750 MHz at the Advanced Magnetic Resonance and Imaging and Spectroscopy (AMRIS) Facility in the McKnight Brain Institute at the University of Florida. All NMR data were collected at 4 °C, unless otherwise specified.

One-dimensional (1D) ^{1}H data were collected at 600 MHz with the carrier frequency centered on water and a spectral width of 12.51 ppm covered by 32 768 data points. The water signal was reduced by presaturation during the 1.5 s relaxation delay. The 1D data were processed with XWIN-NMR software (Bruker NMR) using an exponential function with a 0.1 Hz line broadening, zero-filled once to a final data size of 65 536 points, and Fourier transformed. Data were referenced to acetonitrile (1.93 ppm). One-dimensional temperature titration data were recorded from 4 to 40 °C at 4 °C increments. The temperature dependence of each amide peak was determined by plotting the measured frequencies as a function of temperature. Chemical shift changes of all amides were linear over the temperature range investigated, and amide temperature coefficients were determined from the slopes of the best fit lines.

Two-dimensional (2D) ^{1}H NMR data were collected with the same spectral parameters as the 1D data but with 2048 and 256 complex data points in the acquisition and indirect dimensions, respectively. Quadrature detection in the indirect dimension was achieved using States-TPPI.[60] Water in all 2D experiments was reduced using the 3−9−19 watergate sequence.[61] Total correlation spectroscopy (TOCSY)[62] data were recorded with a 60 ms mixing time using the MLEV-17 spinlock sequence.[63] Nuclear Overhauser effect spectroscopy (NOESY)[64] data were recorded with 200, 300, and 400 ms mixing times. Data were processed with NMRPipe[65] by applying a cosine squared window function and zero filling once prior to Fourier transformation and baseline correction. Data were analyzed with the interactive computer program NMRView.[66]

The ^{1}H resonances assignments of the backbone atoms were made using standard TOCSY- and NOESY-based methods.[44] Amino acid spin systems were primarily identified from

TOCSY cross-peak patterns. In particular, the Ala was identified by its single methyl resonance, and the Arg was identified by the multiple characteristic cross-peaks in the amide to aliphatic region. Sequential assignments were made using the *i* to *i* + *1* connectivities in the NOESY spectra. The presence of lactam bridges were confirmed by NOE cross-peaks from the lactam amide protons to α and amide protons of the bridging residue. NOE cross-peak intensities were measured in NMRView, and $^3J_{HNH\alpha}$ values were measured directly from the 1D spectra using xwinnmr software (Bruker).

Computer-Assisted Molecular Modeling (CAMM). (See Supporting Information for data tables.) All conformational modeling was performed using InsightII software (Molecular Simulations Inc, San Diego, CA). Random structures for the peptides were generated and initially energy minimized with the NMR distance and ϕ torsional restraints added as pseudopotentials to the cvff force field. Distances were calibrated using the relationship $r_{ab}^6 = r_{cal}^6 I_{cal}/I_{ab}$, where r_{ab} is the distance between atoms a and b, I_{ab} is the NOESY a to b cross-peak intensity, r_{cal} is a known distance, and I_{cal} is the corresponding intensity of the NOESY calibration cross-peak. The distance used for calibrations was from the Tyr[10] aromatic protons (2.46 Å). Only the interresidue NOE cross-peaks were used as distance restraints in calculations. One (1.0) Å was added to the calculated distances to define the flat bottom potential energy well and allow for conformational averaging. Scalar coupling constants, $^3J_{HNH\alpha}$, were used to restrain ϕ torsion values using the Karplus equation.[46,49] Only values of $^3J_{HNH\alpha} \leq 5$ Hz were used as restraints, and the corresponding ϕ were restrained to −60° with a flat bottomed potential of ±30°.

The restrained molecular dynamics were run for at least 21 ns in a vacuum with a dielectric constant of 4.0 and 500 K using the cvff force field with cross-terms, Morse potentials, and no cutoff distances. History files from the dynamics were written every 10 ps. Two hundred structures from the history file starting at 1 ns and spaced every 100 ps were energy minimized with the NMR restraints using 2000 steps of steepest decent followed by conjugate gradients and Newton−Raphson until a convergence of 0.1 was reached. The conformations that did not converge (five total) were removed from further analysis. The energy minimized structures were checked for NMR restraint violations using PROCHECK-NMR software.[67] Most of the conformations were in agreement with the restraints with no violations. The conformations with violations were limited to no more than two restraints with maximum upperbound violations of 0.7 Å.

The energy minimized structures were grouped into families using the XCluster program.[50] The conformations were clustered using the dihedral angles of the backbone atoms in the ring and grouped into families of related structures. Because each of the three peptides in the study are different, we were unable to cluster them together. Therefore, for each group of related structures with populations greater than 2% of the total, a representative structure were selected for comparison to groups from the other peptides. This was done by creating template peptide sequences of Gly-9 with the dihedral angles measured from the representative structures. The resulting 31 Gly-9 structures were clustered and analyzed as described above.

Abbreviations: ACTH, adrenocorticotropin; AGRP, agouti-related protein; ASP, human agouti protein; BOP, benziotriazolyloxytris(dimethylamino)phosphonium hexafluorophosphate; CAMM, computer-assisted molecular modeling; DCM, dichloromethane; DIC, *N*,*N*′-diisopropylcarbodiimide; DIEA, diisopropylethylamine; DMEM, Dulbecco's modified Eagle's medium; DMF, dimethylformamide; Dpr, diaminopropionic acid; GPCRs, G-protein-coupled receptors; HBTU, *O*-benzotriazolyl-*N*,*N*,*N*′,*N*′-tetramethyluronium hexafluorophosphate; HF, hydrogen fluoride; HOBt, *N*-hydroxybenzotriazole; Hz, hertz; MC1R, melanocortin-1 receptor; α-MSH, α-melanocyte stimulating hormone; MTII, melanotan II; NMR, nuclear magnetic resonance; NOE, nuclear Overhauser effect ; NOESY, nuclear Overhauser enhanced spectroscopy; POMC, proopiomelanocortin; RP-HPLC, reversed-phase high-performance liquid chromatography; TFA, trifluroacetic acid; TOCSY, total correlation spectroscopy.

Acknowledgment. This work has been funded by NIH Grant RO1-DK57080 (C.H.-L.), a University of Florida Opportunity grant to C.H.-L., N.R., and A.S.E., and an NSF CAREER award (A.S.E.). C.H.-L. is a recipient of a Burroughs Wellcome Fund Career Award in the Biomedical Sciences.

Supporting Information Available: Tables listing proton chemical shifts, NMR-derived distance restraints, and backbone dihedral angles. This material is available free of charge via the Internet at http://pubs.acs.org.

References

(1) Shutter, J. R.; Graham, M.; Kinsey, A. C.; Scully, S.; Lüthy, R.; Stark, K. L. Hypothalamic Expression of ART, a Novel Gene Related to Agouti, Is Up-Regulated in Obese and Diabetic Mutant Mice. *Genes Dev*. **1997**, *11*, 593−602.

(2) Ollmann, M. M.; Wilson, B. D.; Yang, Y.-K.; Kerns, J. A.; Chen, Y.; Gantz, I.; Barsh, G. S. Antagonism of Central Melanocortin Receptors in Vitro and in Vivo by Agouti-Related Protein. *Science* **1997**, *278*, 135−138.

(3) Broberger, C.; Johansen, J.; Johansson, C.; Schalling, M.; Hokfelt, T. The Neuropeptide Y/Agouti Gene-related Protein (AGRP) Brain Circuitry In Normal, Anorectic, and Monosodium Glutamate-Treated Mice. *Proc. Natl. Acad. Sci. U.S.A.* **1998**, *95*, 15043−15048.

(4) Haskell-Luevano, C.; Chen, P.; Li, C.; Chang, K.; Smith, M. S.; Cameron, J. L.; Cone, R. D. Characterization of the Neuroanatomical Distribution of Agouti Related Protein (AGRP) Immunoreactivity in the Rhesus Monkey and the Rat. *Endocrinology* **1999**, *140*, 1408−1415.

(5) Vink, T.; Hinney, A.; van Elburg, A. A.; van Goozen, S. H.; Sandkuijl, L. A.; Sinke, R. J.; Herpertz-Dahlmann, B. M.; Hebebrand, J.; Remschmidt, H.; van Engeland, H.; Adan, R. A. Association between an Agouti-Related Protein Gene Polymorphism and Anorexia Nervosa. *Mol. Psychiatry* **2001**, *6*, 325−328.

(6) Yang, Y.-K.; Thompson, D. A.; Dickinson, C. J.; Wilken, J.; Barsh, G. S.; Kent, S. B. H.; Gantz, I. Characterization of Agouti-Related Protein Binding to Melanocortin Receptors. *Mol. Endocrinol.* **1999**, *13*, 148−155.

(7) Graham, M.; Shutter, J. R.; Sarmiento, U.; Sarosi, I.; Stark, K. L. Overexpression of AGRT Leads to Obesity in Transgenic Mice. *Nat. Genet.* **1997**, *17*, 273−274.

(8) Chhajlani, V.; Wikberg, J. E. S. Molecular Cloning and Expression of the Human Melanocyte Stimulating Hormone Receptor cDNA. *FEBS Lett.* **1992**, *309*, 417−420.

(9) Mountjoy, K. G.; Robbins, L. S.; Mortrud, M. T.; Cone, R. D. The Cloning of a Family of Genes That Encode the Melanocortin Receptors. *Science* **1992**, *257*, 1248−1251.

(10) Roselli-Rehfuss, L.; Mountjoy, K. G.; Robbins, L. S.; Mortrud, M. T.; Low, M. J.; Tatro, J. B.; Entwistle, M. L.; Simerly, R. B.; Cone, R. D. Identification of a Receptor for γ Melanotropin and Other Proopiomelanocortin Peptides in the Hypothalamus and Limbic System. *Proc. Natl. Acad. Sci. U.S.A.* **1993**, *90*, 8856−8860.

(11) Mountjoy, K. G.; Mortrud, M. T.; Low, M. J.; Simerly, R. B.; Cone, R. D. Localization of the Melanocortin-4 Receptor (MC4−R) in Neuroendocrine and Autonomic Control Circuits in the Brain. *Mol. Endocrinol.* **1994**, *8*, 1298−1308.

(12) Gantz, I.; Konda, Y.; Tashiro, T.; Shimoto, Y.; Miwa, H.; Munzert, G.; Watson, S. J.; DelValle, J.; Yamada, T. Molecular Cloning of a Novel Melanocortin Receptor. *J. Biol. Chem.* **1993**, *268*, 8246−8250.

(13) Gantz, I.; Miwa, H.; Konda, Y.; Shimoto, Y.; Tashiro, T.; Watson, S. J.; DelValle, J.; Yamada, T. Molecular Cloning, Expression, and Gene Localization of a Fourth Melanocortin Receptor. *J. Biol. Chem.* **1993**, *268*, 15174−15179.

(14) Gantz, I.; Shimoto, Y.; Konda, Y.; Miwa, H.; Dickinson, C. J.; Yamada, T. Molecular Cloning, Expression, and Characterization of a Fifth Melanocortin Receptor. *Biochem. Biophys. Res. Commun.* **1994**, *200*, 1214−1220.

(15) Cone, R. D.; Lu, D.; Kopula, S.; Vage, D. I.; Klungland, H.; Boston, B.; Chen, W.; Orth, D. N.; Pouton, C.; Kesterson, R. A. The Melanocortin Receptors: Agonists, Antagonists, and the Hormonal Control of Pigmentation. *Recent Prog. Horm. Res.* **1996**, *51*, 287−318.

(16) Lu, D.; Väge, D. I.; Cone, R. D. A Ligand-Mimetic Model for Constitutive Activation of the Melanocortin-1 Receptor. *Mol. Endocrinol.* **1998**, *12*, 592−604.
(17) Chen, A. S.; Marsh, D. J.; Trumbauer, M. E.; Frazier, E. G.; Guan, X. M.; Yu, H.; Rosenblum, C. I.; Vongs, A.; Feng, Y.; Cao, L.; Metzger, J. M.; Strack, A. M.; Camacho, R. E.; Mellin, T. N.; Nunes, C. N.; Min, W.; Fisher, J.; Gopal-Truter, S.; MacIntyre, D. E.; Chen, H. Y.; Van Der Ploeg, L. H. Inactivation of the Mouse Melanocortin-3 Receptor Results in Increased Fat Mass and Reduced Lean Body Mass. *Nat. Genet.* **2000**, *26*, 97−102.
(18) Butler, A. A.; Kesterson, R. A.; Khong, K.; Cullen, M. J.; Pelleymounter, M. A.; Dekoning, J.; Baetscher, M.; Cone, R. D. A Unique Metabolic Syndrome Causes Obesity in the Melanocortin-3 Receptor-Deficient Mouse. *Endocrinology* **2000**, *141*, 3518−3521.
(19) Fan, W.; Boston, B. A.; Kesterson, R. A.; Hruby, V. J.; Cone, R. D. Role of Melanocortinergic Neurons in Feeding and the *Agouti* Obesity Syndrome. *Nature* **1997**, *385*, 165−168.
(20) Huszar, D.; Lynch, C. A.; Fairchild-Huntress, V.; Dunmore, J. H.; Smith, F. J.; Kesterson, R. A.; Boston, B. A.; Fang, Q.; Berkemeir, L. R.; Gu, W.; Cone, R. D.; Campfield, L. A.; Lee, F. Targeted Disruption of the Melanocortin-4 Receptor Results in Obesity in Mice. *Cell* **1997**, *88*, 131−141.
(21) Chhajlani, V.; Muceniece, R.; Wikberg, J. E. S. Molecular Cloning of a Novel Human Melanocortin Receptor. *Biochem. Biophys. Res. Commun.* **1993**, *195*, 866−873.
(22) Chen, W.; Kelly, M. A.; Opitz-Araya, X.; Thomas, R. E.; Low, M. J.; Cone, R. D. Exocrine Gland Dysfunction in MC5-R Deficient Mice: Evidence for Coordinated Regulation of Exocrine Gland Functions by Melanocortin Peptides. *Cell* **1997**, *91*, 789−798.
(23) Miller, M. W.; Duhl, D. M.; Vrieling, H.; Cordes, S. P.; Ollmann, M. M.; Winkes, B. M.; Barsh, G. S. Cloning of the Mouse Agouti Gene Predicts a Secreted Protein Ubiquitously Expressed in Mice Carrying the Lethal Yellow Mutation. *Genes Dev.* **1993**, *7*, 454−467.
(24) Lu, D.; Willard, D.; Patel, I. R.; Kadwell, S.; Overton, L.; Kost, T.; Luther, M.; Chen, W.; Yowchik, R. P.; Wilkison, W. O.; Cone, R. D. Agouti Protein Is an Antagonist of the Melanocyte-Stimulating-Hormone Receptor. *Nature* **1994**, *371*, 799−802.
(25) Bultman, S. J.; Michaud, E. J.; Woychick, R. P. Molecular Characterization of the Mouse Agouti Locus. *Cell* **1992**, *71*, 1195−1204.
(26) Kiefer, L. L.; Ittoop, O. R.; Bunce, K.; Truesdale, A. T.; Willard, D. H.; Nichols, J. S.; Blanchard, S. G.; Mountjoy, K.; Chen, W. J.; Wilkison, W. O. Mutations in the Carboxyl Terminus of the Agouti Protein Decrease Agouti Inhibition of Ligand Binding to the Melanocortin Receptors. *Biochemistry* **1997**, *36*, 2084−2090.
(27) Perry, W. L.; Nakamura, T.; Swing, D. A.; Secrest, L.; Eagleson, B.; Hustad, C. M.; Copeland, N. G.; Jenkins, N. A. Coupled Site-Directed Mutagenesis/Transgenesis Identifies Important Functional Domains of the Mouse Agouti Protein. *Genetics* **1996**, *144*, 255−264.
(28) Willard, D. H.; Bodnar, W.; Harris, C.; Kiefer, L.; Nichols, J. S.; Blanchard, S.; Hoffman, C.; Moyer, M.; Burkhart, W.; Weiel, J.; Luther, M. A.; Wilkison, W. O.; Rocque, W. J. Agouti Structure and Function: Characterization of a Potent α-Melanocyte Stimulating Hormone Receptor Antagonist. *Biochemistry* **1995**, *34*, 12341−12346.
(29) Perry, W. L.; Hustad, C. M.; Swing, D. A.; Jenkins, N. A.; Copeland, N. G. A Transgenic Mouse Assay for Agouti Protein Activity. *Genetics* **1995**, *140*, 267−274.
(30) Quillan, J. M.; Sadee, W.; Wei, E. T.; Jimenez, C.; Ji, L.; Chang, J. K. A Synthetic Human Agouti-Related Protein-(83−132)-NH_2 Fragment Is a Potent Inhibitor of Melanocortin Receptor Function. *FEBS Lett.* **1998**, *428*, 59−62.
(31) Bures, E. J.; Hui, J. O.; Young, Y.; Chow, D. T.; Katta, V.; Rohde, M. F.; Zeni, L.; Rosenfeld, R. D.; Stark, K. L.; Haniu, M. Determination of Disulfide Structure in Agouti-Related Protein (AGRP) by Stepwise Reduction and Alkylation. *Biochemistry* **1998**, *37*, 12172−12177.
(32) Kiefer, L. L.; Veal, J. M.; Mountjoy, K. G.; Wilkison, W. O. Melanocortin Receptor Binding Determinants in the Agouti Protein. *Biochemistry* **1998**, *37*, 991−997.
(33) Bolin, K. A.; Anderson, D. J.; Trulson, J. A.; Thompson, D. A.; Wilken, J.; Kent, S. B.; Gantz, I.; Millhauser, G. L. NMR Structure of a Minimized Human Agouti Related Protein Prepared by Total Chemical Synthesis. *FEBS Lett.* **1999**, *451*, 125−131.
(34) Klemes, D. G.; Kreutzfeld, K. L.; Hadley, M. E.; Cody, W. L.; Hruby, V. J. Potent and prolonged melanotropic activities of the α-MSH fragment analogue, Ac-[Nle,[4] *D*-Phe[7]-α-MSH4-9-NH_2. *Biochem. Biophys. Res. Commun.* **1986**, *137*, 722−728.
(35) (35) Hruby, V. J.; Wilkes, B. C.; Hadley, M. E.; Al-Obeidi, F.; Sawyer, T. K.; Staples, D. J.; DeVaux, A.; Dym, O.; Castrucci, A. M.; Hintz, M. F.; Riehm, J. P.; Rao, K. R. a-Melanotropin: The Minimal Active Sequence in the Frog Skin Bioassay. *J. Med. Chem.* **1987**, *30*, 2126−2130.
(36) **(36)** Castrucci, A. M. L.; Hadley, M. E.; Sawyer, T. K.; Wilkes, B. C.; Al-Obeidi, F.; Staples, D. J.; DeVaux, A. E.; Dym, O.; Hintz, M. F.; Riehm, J.; Rao, K. R.; Hruby, V. J. α-Melanotropin: The Minimal Active Sequence in the Lizard Skin Bioassay. *Gen. Comput. Endocrinol.* **1989**, *73*, 157−163.
(37) Haskell-Luevano, C.; Sawyer, T. K.; Hendrata, S.; North, C.; Panahinia, L.; Stum, M.; Staples, D. J.; Castrucci, A. M.; Hadley, M. E.; Hruby, V. J. Truncation Studies of α-Melanotropin Peptides Identifies Tripeptide Analogues Exhibiting Prolonged Agonist Bioactivity. *Peptides* **1996**, *17*, 995−1002.
(38) Eberle, A. N. *The Melanotropins: Chemistry, Physiology and Mechanisms of Action*; Karger: Basel, 1988.
(39) Schiöth, H. B.; Muceniece, R.; Larsson, M.; Mutulis, F.; Szardenings, M.; Prusis, P.; Lindeberg, G.; Wikberg, J. E. S. Binding of Cyclic and Linear MSH Core Peptides to the Melanocortin Receptor Subtypes. *Eur. J. Pharm.* **1997**, *319*, 369−373.
(40) Haskell-Luevano, C.; Holder, J. R.; Monck, E. K.; Bauzo, R. M. Characterization of Melanocortin NDP-MSH Agonist Peptide Fragments at the Mouse Central and Peripheral Melanocortin Receptors. *J. Med. Chem.* **2001**, *44*, 2247−2252.
(41) Yang, Y.; Fong, T. M.; Dickinson, C. J.; Mao, C.; Li, J. Y.; Tota, M. R.; Mosley, R.; Van Der Ploeg, L. H.; Gantz, I. Molecular Determinants of Ligand Binding to the Human Melanocortin-4 Receptor. *Biochemistry* **2000**, *39*, 14900−14911.
(42) Haskell-Luevano, C.; Monck, E. K.; Wan, Y. P.; Schentrup, A. M. The Agouti-Related Protein Decapeptide (Yc[CRFFNAFC]Y) Possesses Agonist Activity at the Murine Melanocortin-1 Receptor. *Peptides* **2000**, *21*, 683−689.
(43) Tota, M. R.; Smith, T. S.; Mao, C.; MacNeil, T.; Mosley, R. T.; Van der Ploeg, L. H. T.; Fong, T. M. Molecular Interaction of Agouti Protein and Agouti-Related Protein with Human Melanocortin Receptors. *Biochemistry* **1999**, *38*, 897−904.
(44) Wüthrich, K. *NMR of Proteins and Nucleic Acids*; John Wiley & Sons: New York, 1986.
(45) Wishart, D. S.; Sykes, B. D. Chemical Shifts as a Tool for Structure Determination. *Methods Enzymol.* **1994**, *239*, 363−92.
(46) Karplus, M. Contact Electron-Spin Coupling of Nuclear Magnetic Moments. *J. Chem. Phys.* **1959**, *30*, 11−15.
(47) Ohnishi, M.; Urry, D. W. Temperature Dependence of Amide Proton Chemical Shifts-Secondary Structures of Gramicidin S and Valinomycin. *Biochem. Biophys. Res. Commun.* **1969**, *36*, 194−202.
(48) Dyson, H. J.; Rance, M.; Houghten, R. A.; Lerner, R. A.; Wright, P. E. Folding of immunogenic peptide fragments of proteins in water solution. I. Sequence requirements for the formation of a reverse turn. *J. Mol. Biol.* **1988**, *201*, 161−200.
(49) Edison, A. S.; Markley, J. L.; Weinhold, F. Calculations of One-, Two- and Three-Bond Nuclear Spin−Spin Couplings in a Model Peptide and Correlations with Experimental Data. *J. Biomol. NMR* **1994**, *4*, 519−542.
(50) Shenkin, P. S.; McDonald, D. Q. Cluster Analysis of Molecular Conformations. *J. Comput. Chem.* **1994**, *15*, 899−916.
(51) Al-Obeidi, F.; Hruby, V. J.; Hadley, M. E.; Sawyer, T. K.; Castrucci, A. M. D. L. Design, Synthesis, and Biological Activities of a Potent and Selective α-Melanotropin Antagonist. *Int. J. Pept. Protein Res.* **1990**, *35*, 228−234.
(52) Jayawickreme, C. K.; Quillan, M.; Graminski, G. F.; Lerner, M. R. Discovery and Structure−Function Analysis of α-Melanocyte-Stimulating Hormone Antagonists. *J. Biol. Chem.* **1994**, *269*, 29846−29854.
(53) Quillan, J. M.; Jayawickreme, C. K.; Lerner, M. R. Combinatorial Diffusion Assay Used To Identify Topically Active Melanocyte-Stimulating Hormone Receptor Antagonists. *Proc. Natl. Acad. Sci. U.S.A.* **1995**, *92*, 2894−2898.
(54) Hruby, V. J.; Lu, D.; Sharma, S. D.; Castrucci, A. M. L.; Kesterson, R. A.; Al-Obeidi, F. A.; Hadley, M. E.; Cone, R. D. Cyclic Lactam α-Melanotropin Analogues of Ac−Nle[4]-c[Asp[5], *D*Phe[7], Lys[10]]-α-MSH(4−10)-NH_2 with Bulky Aromatic Amino Acids at Position 7 Show High Antagonist Potency and Selectivity at Specific Melanocortin Receptors. *J. Med. Chem.* **1995**, *38*, 3454−3461.
(55) Stewart, J. M.; Young, J. D. *Solid-Phase Peptide Synthesis;* 2nd ed.; Pierce Chemical Co.: Rockford, IL, 1984.
(56) Kaiser, E.; Colescott, R. L.; Bossinger, C. D.; Cook, P. I. Color Test for Detection of Free Terminal Amino Groups in the Solid-Phase Synthesis of Peptides. *Anal. Biochem.* **1970**, *34*, 595−598.
(57) Haskell-Luevano, C.; Cone, R. D.; Monck, E. K.; Wan, Y.-P. Structure Activity Studies of the Melanocortin-4 Receptor by in Vitro Mutagenesis: Identification of Agouti-Related Protein (AGRP), Melanocortin Agonist and Synthetic Peptide Antagonist Interaction Determinants. *Biochemistry* **2001**, *40*, 6164−6179.
(58) Chen, W.; Shields, T. S.; Stork, P. J. S.; Cone, R. D. A Colorimetric Assay for Measuring Activation of Gs- and Gq-Coupled Signaling Pathways. *Anal. Biochem.* **1995**, *226*, 349−354.
(59) Schild, H. O. pA, A New Scale for the Measurement of Drug Antagonism. *Br. J. Pharmacol.* **1947**, *2*, 189−206.

(60) Marion, D.; Ikura, M.; Tschudin, R.; Bax, A. Rapid Recording of 2D NMR Spectra Without Phase Cycling: Application to the Study of Hydrogen Exchange in Proteins. *J. Magn. Reson.* **1989**, *85*, 393−399.
(61) Piotto, M.; Saudek, V.; Sklenar, V. Gradient-tailored Excitation for Single-Quantum NMR Spectroscopy of Aqueous Solutions. *J. Biomol. NMR* **1992**, *2*, 661−666.
(62) Braunschweiler, L.; Ernst, R. R. Coherence Transfer by Isotropic Mixing: Application to Protein Correlation Spectroscopy. *J. Magn. Reson.* **1983**, *53*, 521−528.
(63) Bax, A.; Davis, D. G. MLEV-17-Based Two-Dimensional Homonuclear Magnetization Transfer Spectroscopy. *J. Magn. Reson.* **1985**, *65*, 355−360.
(64) Kumar, A.; Ernst, R. R.; Wuthrich, K. A Two-dimensional Nuclear Overhauser Enhancement (2D NOE) Experiment for the Elucidation of Complete Proton−Proton Cross-Relaxation Networks in Biological Macromolecules. *Biochem. Biophys. Res. Commun.* **1980**, *95*, 1−6.
(65) Delaglio, F.; Grzesiek, S.; Vuister, G. W.; Zhu, G.; Pfeifer, J.; Bax, A. NMR Pipe: a Multidimensional Spectral Processing System Based on UNIX Pipes. *J. Biomol. NMR* **1995**, *6*, 277−293.
(66) Johnson, B. A.; Blevins, R. A. NMR View-A Computer Program for the Visualization and Analysis of NMR Data. *J. Biomol. NMR* **1994**, *4*, 603−614.
(67) Laskowski, R. A.; Rullmannn, J. A.; MacArthur, M. W.; Kaptein, R.; Thornton, J. M. AQUA and PROCHECK−NMR: Programs for Checking the Quality of Protein Structures Solved by NMR. *J. Biomol. NMR* **1996**, *8*, 477−86.

JM010215Z